

Signatures of canted antiferromagnetism in infinite-layer nickelates studied by x-ray magnetic dichroism

G. Krieger,¹ H. Sahib,¹ F. Rosa,² M. Rath,³ Y. Chen,³ A. Raji,^{4,5} P.V.B. Pinho,⁶
C. Lefevre,¹ G. Ghiringhelli,² A. Gloter,⁴ N. Viart,¹ M. Salluzzo,³ and D. Preziosi^{1,*}

¹*Université de Strasbourg, CNRS, IPCMS UMR 7504, F-67034 Strasbourg, France*[†]

²*Dipartimento di Fisica, Politecnico di Milano, Piazza Leonardo da Vinci 32, I-20133 Milano, Italy*

³*CNR-SPIN Complesso di Monte S. Angelo, via Cinthia - I-80126 Napoli, Italy*

⁴*Laboratoire de Physique des Solides, CNRS, Université Paris-Saclay, 91405 Orsay, France*

⁵*Synchrotron SOLEIL, L'Orme des Merisiers, BP 48 St Aubin, 91192 Gif sur Yvette, France*

⁶*ESRF, The European Synchrotron, 71 Avenue des Martyrs, F-38043 Grenoble, France*

We report an experimental study of the magnetic properties of infinite-layer $\text{Nd}_{1-x}\text{Sr}_x\text{NiO}_2$ ($x = 0$ and 0.2) thin films by x-ray magnetic circular dichroism (XMCD) at Ni $L_{3,2}$ - and Nd $M_{5,4}$ -edges. We show that at low temperatures the out-of-plane component of the Ni^{1+} spin-moment is characterized by a rapid increase for magnetic fields below $1T$, followed by a slower linear increase reaching a spin-moment value of $0.25 \mu_B/\text{Ni}$ at $9T$ in the case of superconducting $\text{Nd}_{0.8}\text{Sr}_{0.2}\text{NiO}_2$. On the other hand, the Nd $M_{5,4}$ XMCD shows a clear paramagnetic behaviour, which make both Ni- and Nd-spin-sublattices fully uncorrelated. The magnetic field and temperature dependencies of the Ni $L_{3,2}$ XMCD data can be explained by assuming an out-of-plane canting of the strongly in-plane anti-ferromagnetic ordered Ni^{1+} spins. A symmetry lowering of the NiO_2 planes observed via four-dimensional scanning transmission electron microscopy, triggering a Dzyaloshinskii–Moriya interaction, can be responsible of the proposed Ni^{1+} -spin canting at zero-field. The resulting out-of-plane weak-ferromagnetic coupling under magnetic field explains the relatively large spin-moment and its magnetic field and temperature dependence.

The recent discovery of superconductivity in infinite-layer nickelate thin films [1] is shedding new light on the so-long-sought path towards the understanding of high-temperature superconductivity. Most of the ongoing research is devoted at evidencing differences and similarities between cuprates and infinite-layer nickelates, which share the same square-planar structure and $3d^9$ -electron count. An important question yet to be settled is the difference in the magnetic ground-state, in view of the apparent absence of long-range antiferromagnetic (AFM) order in undoped polycrystalline NdNiO_2 [2, 3] and LaNiO_2 [4–6] samples. The results were initially attributed to local oxygen non-stoichiometry and Ni^{2+} -related defects besides the possible presence of ferromagnetic impurities, which, would explain also the absence of bulk superconductivity [3]. Theoretically, most of the studies suggest that the energetically-favored AFM order of the Ni $3d^9$ system is more unstable than in cuprates, in particular when considering the role of the rare-earth magnetism [7–10](plus ref. therein). Indeed, G-type and C-type AFM ground states are found very close in energy, and Sr-doping has been predicted to favor also a transition from G-AFM towards C-AFM [10]. Concerning infinite-layer nickelate thin films, only few studies explicitly addressing the magnetism are available [11–13]. This is particularly relevant, as the electronic properties of thin films can be different from bulk samples. Resonant inelastic x-ray scattering (RIXS) experiments in epitaxial films show dispersing magnetic excitations within the NiO_2 planes, analogous to that of doped cuprates, but with a next-neighbour AFM exchange coupling only half

the value found in cuprates [14]. Sr-doping, while triggering superconductivity, gives rise to a flattening-out of the magnon-excitation [11]. Muon-spin rotation/relaxation measurements on SrTiO_3 -capped undoped and superconducting $\text{R}_{1-x}\text{Sr}_x\text{NiO}_2$ thin films ($R = \text{Nd, Pr and La}$), revealed a complex spin-dynamics, with a temperature dependence of the spin-susceptibility pointing to some kind of intrinsic magnetic order, attributed to the Ni-spin-sublattice, despite the magnetism stemming from the R $4f$ -states in some sample series [12]. Noteworthy, none of these studies could explicitly address separately the magnetism of the Ni^{1+} and R sublattices, nor single out the contributions from unwanted impurities and from Ni-ions with a $2+$ valence state that could be present due to an incomplete oxygen reduction, as highlighted in recent works [15, 16].

Here, we report a study of the intrinsic magnetic properties of the Ni^{1+} -spin-sublattice in Nd-based infinite-layer thin films, by performing element(and valence)-specific x-ray magnetic circular dichroism (XMCD) experiments at the Ni $L_{3,2}$ - and Nd $M_{5,4}$ -edges as a function of magnetic field (H) and temperatures (T) on a series of $\text{Nd}_{1-x}\text{Sr}_x\text{NiO}_2$ ($x = 0$ and 0.2) samples. We find evidences of AFM-correlations in the Ni^{1+} -spin-sublattice, but at the same time a large, field induced, Ni^{1+} out-of-plane spin-moment a factor 10 larger than the canted Cu^{2+} spin-moment determined by XMCD in cuprates[17]. All the samples were grown onto (001) SrTiO_3 (STO) single-crystals, with/without a STO capping-layer and the latter, when present, was only three-unit-cells thick (~ 1 nm). Details about the

growth, structural and transport characterizations are provided elsewhere [18]. The experiments were performed at DEIMOS and ID32 beamlines of the SOLEIL and ESRF Synchrotron facilities (France), respectively, in total electron yield (TEY) and in fluorescence yield (FY) modes, with beam size of the order of $500 \times 800 \mu\text{m}^2$, in normal incidence (beam and magnetic field perpendicular to the NiO_2 planes). The Ni-XMCD data analysis was performed by applying the sum-rules to determine the Ni magnetic spin moment ($\text{Ni-}\mu_{\text{spin}}$), by using the nominal values of 1 and 1.2 holes in the $3d$ levels for the Ni^{1+} and $\text{Ni}^{1.2+}$ sites in the respective samples to account for the different Sr-doping. The quadrupole spin moment was considered negligible [19].

First we show below how the XMCD technique is able to differentiate the (intrinsic) magnetic moment of Ni^{1+} and Nd^{3+} ions, from the extrinsic contribution of non ideal-regions where Ni is in a Ni^{2+} valence state. Hereof we show Ni- $L_{3,2}$ edge XAS and XMCD data on a series of STO-capped and uncapped NdNiO_2 thin films in both TEY and FY modes. The XMCD signal is proportional to the magnetic moment of a given ion (here Ni^{1+} , Ni^{2+} and Nd^{3+}) projected along the x-ray beam and the external field. In the TEY mode, the XAS and XMCD spectra have a major contribution from the top-most unit-cells, while in the FY-mode the entire film volume is equally probed. Upper-part of Figures 1a,b shows circular polarized Ni- L_3 edge XAS spectra (average of C-plus and C-minus polarized spectra), normalized to the L_3 -edge intensity, acquired at $H = 9T$ and at $T = 4K$ in normal incidence geometry for both STO-capped and uncapped samples. The Ni- L_2 edges are shown in the related insets. The XAS of uncapped samples are broader than the ones measured in capped samples, due to an important contribution of the higher energy Ni^{2+} feature akin to not fully reduced unit-cells, in agreement with other studies [15, 16]. The higher energy feature should not be compared/confused with the XAS broadening at the Ni- L_3 edge observed upon Sr-doping [20], as the spectral weight of the latter is much less important. Here, the comparison between TEY and FY XAS spectra shows that the Ni^{2+} signal is mainly due to the first surface unit-cells, in agreement with scanning transmission electron microscopy and recent x-ray photoemission spectroscopy measurements [15, 21]. On the other hand, TEY and FY XAS spectra of capped samples largely overlap and show only a Ni^{1+} feature, with only small differences between the two acquisition modes attributed to Ni^{2+} located at the interface with the STO-capping-layer. These experimental evidences demonstrate and confirm that the STO-capping allows a better stabilization of the infinite-layer phase [22].

The differences between XAS spectra of capped and uncapped samples echoed in the XMCD data, shown in the bottom-panel of Figures 1a,b. In particular, uncapped $\text{Nd}_{1-x}\text{Sr}_x\text{NiO}_2$ are characterized by a doublet

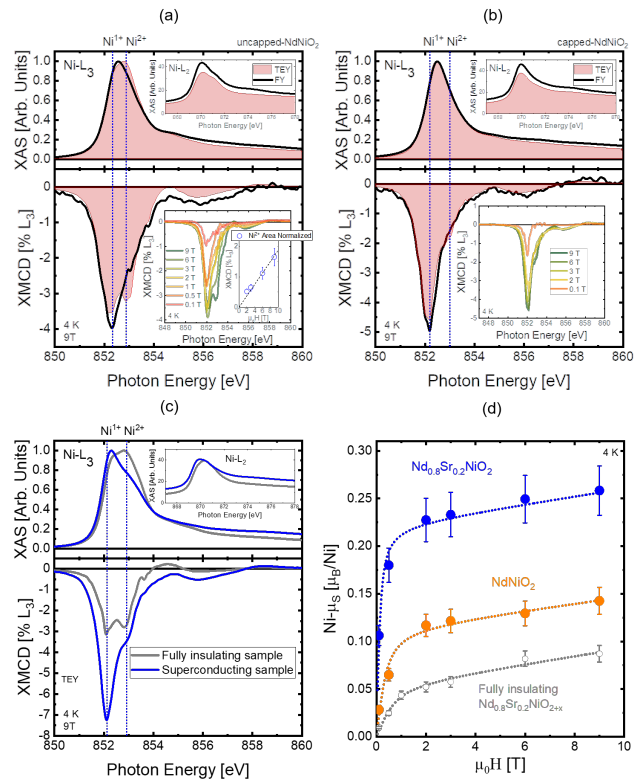


FIG. 1. XAS (top part) and XMCD (bottom part) of (a) uncapped, (b) capped NdNiO_2 and (c) capped $\text{Nd}_{0.8}\text{Sr}_{0.2}\text{NiO}_2$ thin films acquired in TEY and FY modes at $9T$ and $4K$. In (c) we compare data on superconducting $\text{Nd}_{0.8}\text{Sr}_{0.2}\text{NiO}_2$ and poorly reduced non-superconducting $\text{Nd}_{0.8}\text{Sr}_{0.2}\text{NiO}_{2+x}$ thin films. The insets show the Ni L_2 -edges (top panel) together with the H-dependence of the XMCD at the Ni L_3 -edge (bottom panel). In the inset of bottom panel in (a) we show also the XMCD contribution due to the Ni^{2+} fraction observed in uncapped samples. (d) H-dependence of the $\text{Ni-}\mu_{\text{spin}}$ for different capped samples at $4K$. Dotted lines are guide to the eyes.

structure in the TEY-XMCD spectra at $9T$ and $4K$. This doublet almost disappears at low magnetic field (see inset), and it is absent in the FY-XMCD spectra, where a unique peak shows up. As highlighted by the vertical blue dotted lines, the two peaks in the TEY-XMCD doublet corresponds to Ni^{1+} and Ni^{2+} features of the XAS spectra. It is worth noting that the TEY-XMCD peak intensity due to the Ni^{2+} feature, normalized to the overall area of the XMCD at the Ni- L_3 edge, shows a linear H-dependence (see inset of 1a), suggesting a paramagnetic contribution from the incomplete reduction of the surface unit-cells. On the other hand, in both TEY or FY modes, the XMCD intensity at the Ni^{1+} energy dominates over the Ni^{2+} contribution. In the case of the capped samples the FY-XMCD and TEY-XMCD spectra almost overlap, and are characterized by a unique and sharp peak mainly associated to the Ni^{1+} . A small Ni^{2+} shoulder shows up only in the TEY-XMCD spectra

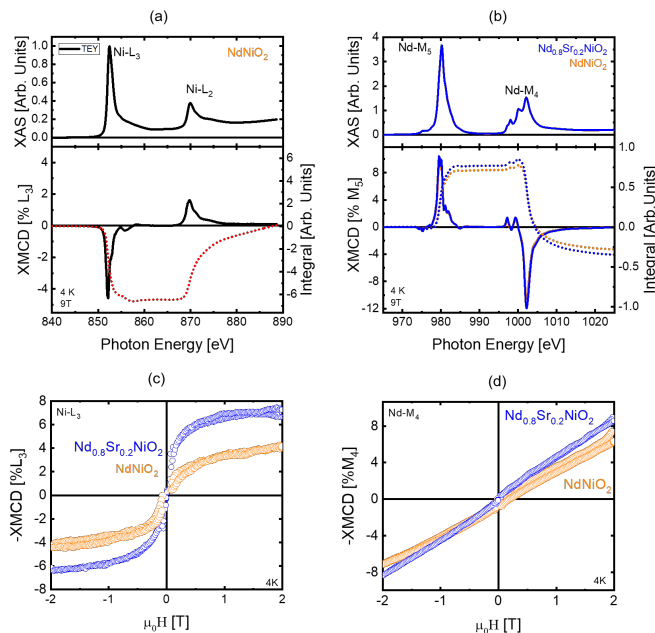


FIG. 2. NdNiO_2 and $\text{Nd}_{0.8}\text{Sr}_{0.2}\text{NiO}_2$ XAS (top-panel) and XMCD (bottom-panel) at the (a) Ni $L_{3,2}$ - and (b) Nd $M_{5,4}$ -edges. The integrals of the XMCD spectra are shown as dotted-lines. Magnetic hysteresis at the (c) Ni L_3 -edge and (d) Nd M_4 peaks, normalized to the pre-edge value for both samples.

and only at high magnetic fields, possibly due to the top-interface unit-cell. Finally, in order to confirm that the large XMCD signal in capped samples is related to Ni^{1+} -spins and it is intrinsic to our infinite-layer thin films, in Figure 1c we show additional XMCD data on an insulating, not fully reduced, $\text{Nd}_{0.8}\text{Sr}_{0.2}\text{NiO}_{2+x}$ sample, realized after a partial topotactic reduction process. As expected, here the XAS spectra are characterized by a more relevant Ni^{2+} peak, a very large doublet in the XMCD signal and correspondingly a factor five lower Ni^{1+} XMCD even at the maximum magnetic field. All this somehow tells that the Ni^{1+} -spins, when arranged in a planar geometry without neighbor apical oxygen ions, exhibit a relatively strong magnetism in Nd-based infinite-layer samples, in qualitative agreement with Fowlie *et al.* [12].

Now we address the magnetic properties of capped samples by discussing the XMCD data as a function of both H and T. In Figure 1d we show the Ni- μ_{spin} H-dependence in the $0.01 - 9T$ range at 4K estimated from the sum-rules applied to the Ni $L_{3,2}$ -edges XMCD spectra of STO-capped NdNiO_2 , $\text{Nd}_{0.8}\text{Sr}_{0.2}\text{NiO}_2$ and defective $\text{Nd}_{0.8}\text{Sr}_{0.2}\text{NiO}_{2+x}$ samples. Interestingly, the Ni- μ_{spin} at 9T is $\sim 0.12\mu_B/\text{Ni}$ and $\sim 0.25\mu_B/\text{Ni}$ for the undoped and superconducting samples, respectively, and $\sim 0.07\mu_B/\text{Ni}$, in defective $\text{Nd}_{0.8}\text{Sr}_{0.2}\text{NiO}_{2+x}$. Moreover, all the samples exhibit a peculiar H-dependence characterized by a rapid increase below 1T followed by a slow linear increase at higher fields. The similar slope at high field for all sam-

ples excludes any role of Ni^{2+} -related defects or ferromagnetic impurities to the magnetism of our samples. In Figures 2a,b we compare the XAS and XMCD spectra acquired in normal incidence and 9T at the Ni $L_{3,2}$ - and Nd $M_{5,4}$ -edges. The Nd $M_{5,4}$ XAS shows typical features of a Nd^{3+} valence state with the XMCD opposite to the Ni $L_{3,2}$ one, as already reported in literature [23]. In Figures 2c,d we show the magnetic field hysteresis loops, obtained by measuring the XMCD at the Ni L_3 (~ 852 eV) and Nd M_4 (~ 981 eV) edges. These data are overall proportional to the Ni^{1+} and Nd^{3+} out-of-plane magnetic moments. The Ni L_3 XMCD loops show apparently no clear hysteresis, and the data perfectly agree with the H-dependence of the Ni- μ_{spin} determined from the sum-rules, again suggesting that the Ni^{1+} intrinsic magnetization is characterized by a very steep increase below 1T followed by an H-linear slow increase for both samples. Moreover, the data confirm that the Ni^{1+} spin-moment is substantially larger for the doped superconducting sample. The Nd M_4 XMCD hysteresis loop, on the other hand, shows a paramagnetic signal fully uncorrelated to the Ni- μ_{spin} H-dependence.

In order to obtain further insights about the magnetic correlations that are at play, we show in Figure 3 the Ni- μ_{spin} T-dependence in undoped and Sr-doped (superconducting and non) samples at field values of 0.1T and 2T. The latter were chosen to get insights from the two different regions of the Ni-spin H-dependence (cf. Fig. 1d). At 2T we find that the Ni- μ_{spin} are slowly increasing for decreasing temperatures obeying with a good accuracy to a Curie-Weiss-law in the entire T-range, and pointing towards magnetic correlations exemplary of a frustrated system with weak-FM coupling in the out-of-plane direction with respect to the NiO_2 planes (Fig. 3a). This tells that magnetic correlations among Ni^{1+} -spins are also present along this specific direction which confirms recent theoretical calculations [9]. The situation in the very weak-field (0.1T) is slightly different. The superconducting sample exhibits in the region between 50K and 100K a small deviation from the Curie-Weiss behaviour, while the undoped sample, below 50K, shows a reduction of the Ni- μ_{spin} moment suggesting the presence of AFM correlations.

To explain the origin of this large field-induced Ni- μ_{spin} we consider a canted (G-type) AFM spin ordering as sketched in the inset of Figure 3b. The canting of the Ni^{1+} spins is, for sake of simplicity, represented in the xz plane. At zero field the out-of-plane spin moment is null. Upon H-increasing, the intrinsic magnetic instability of the Ni-spin-sublattice, associated to a weak out-of-plane AFM coupling, allows a partial spin-flip of the (canted) spins, with consequent alignment along the field and the emergence of a non zero Ni- μ_{spin} out-of-plane component. In particular, the canted component reaches its maximum with the applied field of approximately 1T. This canted spin-moment is somewhat locked

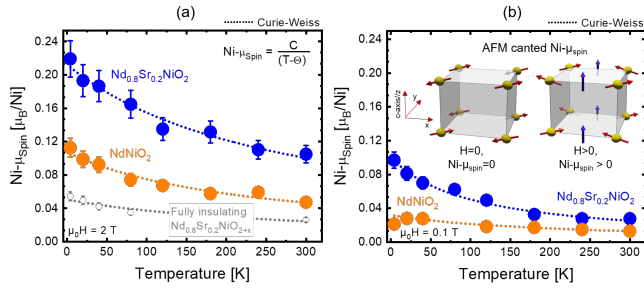


FIG. 3. Temperature dependence of the $\text{Ni-}\mu_{spin}$ for different samples acquired at (a) $2T$ and (b) $0.1T$. Dotted lines represent fit to the data via Curie-Weiss-law. The cartoons sketch the canted-AFM spin arrangement within the NiO_2 planes.

to the in-plane AFM order. At $0.1T$, the temperature dependence of the magnetic moment reflects the in-plane AFM-order in NdNiO_2 , giving rise to a decrease of the $\text{Ni-}\mu_{spin}$ out-of-plane component below 50 K, as shown in Figure 3b. In Sr-doped sample, where magnetic excitations are strongly damped and AFM-correlations are short-range, a larger canted magnetic component is observed at $0.1T$ (Fig. 1d) and the temperature dependence of the $\text{Ni-}\mu_{spin}$ out-of-plane component shows only a small deviation from a Curie-Weiss law. The slow linear increase above $1T$ is presumably due to a very small and slow increase of spin-canting angle, because the in-plane AFM coupling is very strong.

While this model can simultaneously explain the presence of in-plane AFM-correlations and the relative large H-induced spin-moment, the origin of the spin-canting has to be settled. Our XMCD data clearly demonstrate that the measured magnetic moment should be attributed to Ni^{1+} in the NiO_2 planes. However, perfectly arranged square-planar NiO_2 would not give rise to an out-of-plane spin-canting due to the lack of the apical oxygen, as for Cu^{2+} in the case of $\text{Sr}_2\text{CuO}_2\text{Cl}_2$ oxychloride cuprate. On the other hand, a canted spin-moment was observed in the $\text{La}_{2-x}\text{Sr}_x\text{CuO}_4$ and $\text{R}_1\text{Ba}_2\text{Cu}_3\text{O}_7$ families, and attributed to the Dzyaloshinskii–Moriya interaction (DMI) [17] (and references therein) taking place due to non-perfectly square-planar Cu-O-Cu bonds, thus to a lowering of the symmetry. In doped and superconducting $\text{La}_{2-x}\text{Sr}_x\text{CuO}_4$ and $\text{R}_1\text{Ba}_2\text{Cu}_3\text{O}_7$, the weak-ferromagnetic out-of-plane component has a pure paramagnetic temperature and magnetic field dependence, while in undoped $\text{La}_2\text{SrCuO}_4$ the temperature dependence reflects the in-plane AFM long-range order.

Proceeding in analogy with cuprates, we tried to identify any (structural) sources of the spin-canting in our NdNiO_2 by using the divergence of the Center of Mass (dCoM) four-dimensional (4D) scanning transmission electron microscopy (STEM-dCOM) technique. The dCoM 4D-STEM technique has the unique capability to image the oxygen-ion positions with high accuracy. Fig-

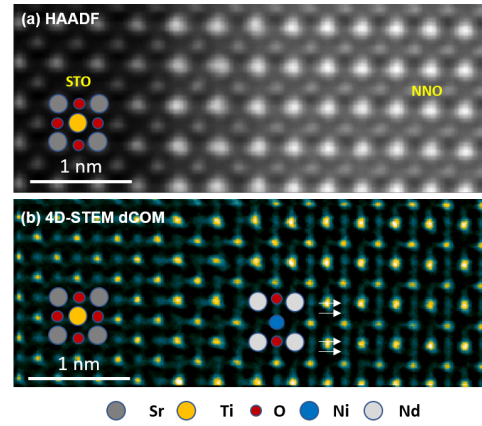


FIG. 4. (a) High-angle annular dark-field imaging (HAADF) of capped NNO sample acquired at 300K combined to a (b) dCOM 4D-STEM imaging showing the NiO_2 planes. The presence of oxygen-ions along the Ni-O-Ni bond with different center of mass positions are indicated by the arrows.

ures 4a,b show high-angle annular dark field STEM and dCOM 4D-STEM map images, respectively, along the $[100]$ cubic axis of STO, on an undoped, capped NdNiO_2 film. The NiO_4 square-planar coordination is altered and presents an apparent oxygen-doubling with a zig-zag pattern, as indicated by the white arrows in 4b. The presence of an additional (faded) oxygen along the Ni-O-Ni bond suggests that the oxygen ions are not exactly at the center. From the data, we cannot exactly identify the source of this non-ideal planar-configuration. We cannot exclude that it originates from tilt/rotation of the NiO_2 bonds and/or to a cation off-centering. Nonetheless, the overall symmetry of the structure appears lowered by these structural distortions, and this can explain the sizable DMI and a non-collinear Ni^{1+} spin arrangement [24].

In conclusion, with our elemental-sensitive X-ray circular magnetic dichroism experiments at the Ni $L_{3,2}$ - and Nd $M_{5,4}$ -edges we could demonstrate that the magnetic properties of Nd-based infinite-layer nickelate parent compound and of superconducting thin films are related to an AFM-canted arrangement of the Ni^{1+} -spin, ruling out the contribution from Ni^{2+} and of extended defects to the sample magnetism. Moreover, we showed that the paramagnetic $\text{Nd}^{3+} 4f$ states do not affect the $\text{Ni-}\mu_{spin}$ $3d$ H-dependence. This finding may question the role of the Nd-Ni hybridization in mediating the out-of-plane exchange interaction [9]. The spin-canting is attributed to non-perfectly square-planar NiO_2 bonding, as evidenced by dCOM-4D-STEM measurements, which lower the symmetry and is responsible for a sizable DMI among the Ni^{1+} .

ACKNOWLEDGMENTS

This work was funded by the French National Research Agency (ANR) through the ANR-JCJC FOXIES ANR-21-CE08-0021. This work was also done as part of the Interdisciplinary Thematic Institute QMat, ITI 2021 2028 program of the University of Strasbourg, CNRS and Inserm, and supported by IdEx Unistra (ANR 10 IDEX 0002), and by SFRI STRAT'US project (ANR 20 SFRI 0012) and EUR QMAT ANR-17-EURE-0024 under the framework of the French Investments for the Future Program. The synchrotron experiments were performed at ESRF and SOLEIL Synchrotron facilities in France under proposal numbers SC-5296 and 20200718, respectively. D.P. acknowledges fruitful discussions with Gabriele de Luca regarding the Nd sum-rules, and Guillaume Rogez for the magnetism in general. André Thiaville is also acknowledged for discussions over the possible presence of DMI in our system.

BIBLIOGRAPHY

* daniele.preziosi@ipcms.unistra.fr

† present address: Eindhoven University of Technology, P.O. Box 513, 5600 MB Eindhoven, The Netherlands

- [1] D. Li, K. Lee, B. Y. Wang, M. Osada, S. Crossley, H. R. Lee, Y. Cui, Y. Hikita, and H. Y. Hwang, Superconductivity in an infinite-layer nickelate, *Nature* **572**, 624 (2019).
- [2] M. A. Hayward and M. J. Rosseinsky, Synthesis of the infinite layer Ni(I) phase NdNiO_{2+x} by low temperature reduction of NdNiO_3 with sodium hydride, *Solid State Sci.* **5**, 839 (2003).
- [3] Q. Li, C. He, J. Si, X. Zhu, Y. Zhang, and H.-H. Wen, Absence of superconductivity in bulk $\text{Nd}_{1-x}\text{Sr}_x\text{NiO}_2$, *Commun. Mater.* **1**, 16 (2020).
- [4] M. A. Hayward, M. A. Green, M. J. Rosseinsky, and J. Sloan, Sodium hydride as a powerful reducing agent for topotactic oxide deintercalation: Synthesis and characterization of the nickel(I) oxide LaNiO_2 , *J. Am. Chem. Soc.* **121**, 8843 (1999).
- [5] R. A. Ortiz, P. Pupal, M. Klett, F. Hotz, R. K. Kremer, H. Trepka, M. Hemmida, H.-A. K. von Nidda, M. Isobe, R. Khasanov, H. Luetkens, P. Hansmann, B. Keimer, T. Schäfer, and M. Hepting, Magnetic correlations in infinite-layer nickelates: An experimental and theoretical multimethod study, *Phys. Rev. Res.* **4**, 23093 (2022).
- [6] D. Zhao, Y. Zhou, Y. Fu, L. Wang, X. Zhou, H. Cheng, J. Li, D. Song, S. Li, B. Kang, L. Zheng, L. Nie, Z. Wu, M. Shan, F. Yu, J. Ying, S. Wang, J. Mei, T. Wu, and X. Chen, Intrinsic spin susceptibility and pseudogaplike behavior in infinite-layer LaNiO_2 , *Physical Review Letters* **126**, 197001 (2021).
- [7] M.-Y. Choi, W. E. Pickett, and K.-W. Lee, Fluctuation-frustrated flat band instabilities in NdNiO_2 , *Phys. Rev. Res.* **2**, 033445 (2020).
- [8] F. Lechermann, Doping-dependent character and possible magnetic ordering of NdNiO_2 , *Physical Review Materials* **5**, 044803 (2021).
- [9] Y. Zhang, X. He, J. Zhang, J. Wang, and P. Ghosez, Incommensurate Magnetic Order in Hole-Doped Infinite-Layer Nickelate Superconductors due to Competing Magnetic Interactions, *Adv. Funct. Mater.* **n/a**, 2304187 (2023).
- [10] A. Sahinovic, B. Geisler, and R. Pentcheva, Nature of the magnetic coupling in infinite-layer nickelates versus cuprates, *Phys. Rev. Mater.* **7**, 114803 (2023).
- [11] H. Lu, M. Rossi, A. Nag, M. Osada, D. F. Li, K. Lee, B. Y. Wang, M. Garcia-Fernandez, S. Agrestini, Z. X. Shen, E. M. Been, B. Moritz, T. P. Devereaux, J. Zaanen, H. Y. Hwang, K.-J. Zhou, and W. S. Lee, Magnetic excitations in infinite-layer nickelates, *Science* **373**, 213 (2021).
- [12] J. Fowlie, M. Hadjimichael, M. M. Martins, D. Li, M. Osada, B. Y. Wang, K. Lee, Y. Lee, Z. Salman, T. Prokscha, J. M. Triscone, H. Y. Hwang, and A. Suter, Intrinsic magnetism in superconducting infinite-layer nickelates, *Nat. Phys.* **18**, 1043 (2022), [arXiv:2201.11943](https://arxiv.org/abs/2201.11943).
- [13] M. Rossi, H. Lu, K. Lee, B. H. Goodge, J. Choi, M. Osada, Y. Lee, D. Li, B. Y. Wang, D. Jost, S. Agrestini, M. Garcia-Fernandez, Z. X. Shen, K.-J. Zhou, E. Been, B. Moritz, L. F. Kourkoutis, T. P. Devereaux, H. Y. Hwang, and W. S. Lee, Universal orbital and magnetic structures in infinite-layer nickelates, *Phys. Rev. B* **109**, 024512 (2024).
- [14] L. Braicovich, L. J. P. Ament, V. Bisogni, F. Forte, C. Aruta, G. Balestrino, N. B. Brookes, G. M. De Luca, P. G. Medaglia, F. M. Granozio, M. Radovic, M. Salluzzo, J. van den Brink, and G. Ghiringhelli, Dispersion of Magnetic Excitations in the Cuprate La_2CuO_4 and CaCuO_2 Compounds Measured Using Resonant X-Ray Scattering, *Physical Review Letters* **102**, 167401 (2009).
- [15] A. Raji, G. Krieger, N. Viart, D. Preziosi, J.-P. Rueff, and A. Gloter, Charge Distribution across Capped and Uncapped Infinite-Layer Neodymium Nickelate Thin Films, *Small*, 2304872 (2023).
- [16] C. T. Parzyck, N. K. Gupta, Y. Wu, V. Anil, L. Bhatt, M. Bouliane, R. Gong, B. Z. Gregory, A. Luo, R. Surtarto, F. He, Y.-D. Chuang, T. Zhou, G. Herranz, L. F. Kourkoutis, A. Singer, D. G. Schlom, D. G. Hawthorn, and K. M. Shen, Absence of $3a_0$ charge density wave order in the infinite-layer nickelate NdNiO_2 , *Nat. Mater.* [10.1038/s41563-024-01797-0](https://doi.org/10.1038/s41563-024-01797-0) (2024).
- [17] G. M. De Luca, G. Ghiringhelli, M. Moretti Sala, S. Di Matteo, M. W. Haverkort, H. Berger, V. Bisogni, J. C. Cezar, N. B. Brookes, and M. Salluzzo, Weak magnetism in insulating and superconducting cuprates, *Phys. Rev. B* **82**, 10.1103/PhysRevB.82.214504 (2010).
- [18] G. Krieger, A. Raji, L. Schlur, G. Versini, C. Bouillet, M. Lenertz, J. Robert, A. Gloter, N. Viart, and D. Preziosi, Synthesis of infinite-layer nickelates and influence of the capping-layer on magnetotransport, *J. Phys. D: Appl. Phys.* **56**, 024003 (2023).
- [19] D. Preziosi, S. Homkar, C. Lefevre, N. Viart, and M. Salluzzo, Unusual anisotropic magnetic orbital moment obtained from x-ray magnetic circular dichroism in a multiferroic oxide system, *Phys. Rev. B* **103**, 184420 (2021).
- [20] M. Rossi, H. Lu, A. Nag, D. Li, M. Osada, K. Lee, B. Y. Wang, S. Agrestini, M. Garcia-Fernandez, Y. D. Chuang,

- Z. X. Shen, H. Y. Hwang, B. Moritz, K.-J. Zhou, T. P. Devereaux, and W. S. Lee, Orbital and Spin Character of Doped Carriers in Infinite-Layer Nickelates, *Phys. Rev. B* **104**, L220505 (2021).
- [21] M. Rath, Y. Chen, G. Krieger, H. Sahib, D. Preziosi, and M. Salluzzo, Scanning tunnelling microscopy and x-ray photoemission studies of NdNiO₂ infinite-layer nickelates films (2024), [arXiv:2402.03143](https://arxiv.org/abs/2402.03143) [[cond-mat.supr-con](https://arxiv.org/abs/2402.03143)].
- [22] K. Lee, B. H. Goodge, D. Li, M. Osada, B. Y. Wang, Y. Cui, L. F. Kourkoutis, and H. Y. Hwang, Aspects of the synthesis of thin film superconducting infinite-layer nickelates, *APL Mater.* **8**, 41107 (2020).
- [23] J. Spring, G. De Luca, S. Jöhr, J. Herrero-Martín, C. Guillemard, C. Piamonteze, C. M. M. Rosário, H. Hilgenkamp, and M. Gibert, Paramagnetic nd sublattice and thickness-dependent ferromagnetism in Nd₂NiMnO₆ double perovskite thin films, *Phys. Rev. Mater.* **7**, 104407 (2023).
- [24] A. Fert, M. Chshiev, A. Thiaville, and H. Yang, From early theories of dzyaloshinskii–moriya interactions in metallic systems to today’s novel roads, *Journal of the Physical Society of Japan* **92**, 081001 (2023).